Hang-Glider Response to Atmospheric Inputs

Guido de Matteis*
University of Rome "La Sapienza," 00184 Rome, Italy

Introduction

THE analysis of the dynamics of hang gliders has been the subject of two recent papers[1,2] in which, respectively, a model of the vehicle was formulated and the response to the control inputs was evaluated. In this framework, the present Note is addressed to the problem of the hang-glider flight in a turbulent atmosphere. Previous studies, based on approximate unsteady aerodynamics and on a very simple approach, already considered the load-factor variation and the vertical displacement experienced by a glider in a sharp edged[3] and sinusoidal gust.[4] Because of the low-speed and low wing-loading, the safety of the hang-glider flight is affected by atmospheric conditions to quite a large extent as confirmed by the accident statistics. In this respect, a general and complete analysis is of interest, where, in analogy with conventional aircraft, the hang-glider response to atmospheric inputs is dealt with in terms of gust transfer functions and power spectral densities (PSD) of the output.

In what follows, our attention is restricted to the longitudinal motion of a standard, rigid hang-glider configuration[1] in a nonuniform atmosphere. The gust transfer functions of the longitudinal state variables and of the load factor are determined. The effects of the approximations connected with the modeling of the inputs are discussed in relation to the characteristic frequencies of the glider in cruise conditions.

Analysis and Discussion

Following the approach given in Refs. 5 and 6, under the hypotheses of ergodic and frozen turbulence and of planar airplane, the sinusoidal turbulent velocity components are expanded into Taylor's series to the first order. As an observation, the condition associated with the frozen field assumption, i.e., $V_e/W > 1/3$, where W is the mean gust velocity and V_e is the flight speed,[6] is rather critical as far as an aircraft having V_e of the order of 10 m/s is dealt with. However, we expect a hang glider not to fly in severe weather conditions so that a low value of W is reasonable.

Thus, after assuming that the effect of the gradient $\partial u_g/\partial x$ is negligible for the tailless hang glider, the perturbation velocity components in the aerodynamic terms of the linear longitudinal equations of motions, in body axes, are written as

$$u'_t = u' + u_g, \qquad w'_t = w' + w_g, \qquad q'_t = q' + q_g$$

where u', w', and q' are the inertial velocity components and the pitch rate, respectively; u_g and w_g are the gust velocity components in the glider's center of mass; and $q_g = \partial w_g/\partial x = j\Omega w_g$, Ω being the longitudinal wave number. The perturbation of the angle of attack is $\alpha'_t = \alpha' - (w_g/V_e)$ and, as far as the unsteady aerodynamics is considered, we write $\dot{\alpha}'_t = \dot{\alpha}' - \dot{\alpha}_g$ and $\dot{q}'_t = \dot{q}' + \dot{q}_g$, where $\dot{\alpha}_g = -q_g$ and $\dot{q}_g = j\Omega V_e q_g$.[5]

For the sake of brevity, the dynamic model of the aircraft is not recalled here and reference is made to Ref. 1 for the detailed formulation of the small-perturbation, Laplace-transformed governing equations.

The response to the atmospheric inputs is, in the frequency domain

$$\bar{x} = G(\hat{s})\bar{x}_g \tag{1}$$

where $\bar{x}^T = (\bar{\hat{u}}', \bar{\hat{w}}', \bar{\theta}')$ and $\bar{x}_g^T = (\bar{\hat{u}}_g, \bar{\hat{w}}_g, \bar{\hat{q}}_g)$ are the perturbed state and gust disturbance vectors, respectively. The caret and overbars indicate dimensionless and Laplace-transformed quantities, respectively. The transfer functions matrix $G(\hat{s})$ is

$$G(\hat{s}) = A^{-1}(\hat{s})B(\hat{s}) \tag{2}$$

where A is the characteristic matrix of the system (Table 1 of Ref. 1, for the fixed control case) and B is

$$B = \begin{bmatrix} -2\hat{u}_e C_{x_e} & C_{z_\alpha} - 2\hat{u}_e C_{x_e} & 2\mu\hat{w}_e - C^W_{x_q} + C^W_{x_{\dot{\alpha}}} \\ -2\hat{w}_e C_{z_e} & C_{z_\alpha} - 2\hat{w}_e C_{x_e} & 2\mu\hat{u}_e - C^W_{z_q} + C^W_{z_{\dot{\alpha}}} - C_{z_{\dot{q}}}\hat{s} \\ \begin{matrix} -\hat{u}_e(2C^W_{m_e} + \hat{z}^C_e C_{x_e} \\ -\hat{x}^C_e C_{z_e} + \hat{z}^P_e C^P_{x_e} \\ -\hat{x}^P_e C^P_{z_e}) \end{matrix} & \begin{matrix} 1/2(\hat{z}^C_e C^W_{x_\alpha} - \hat{x}^C_e C^W_{x_\alpha} + \hat{x}^P_e C^P_{x_\alpha} \\ -\hat{x}^P_e C^P_{z_\alpha} + 2C^W_{m_\alpha}) - \hat{w}_e(2C^W_{m_e} \\ +\hat{z}^C_e C^W_{x_e} - \hat{x}^C_e C^W_{z_e} + \hat{z}^P_e C^P_{x_e} - \hat{x}^P_e C^P_{z_e}) \end{matrix} & \begin{matrix} -1/2(\hat{z}^C_e C^W_{x_q} - \hat{x}^C_e C^W_{z_q} + 2C^W_{m_q} \\ -2C^W_{m_{\dot{\alpha}}} - \hat{z}^C_e C^C_{x_{\dot{\alpha}}} + \hat{x}^C_e C^C_{z_{\dot{\alpha}}}) \\ +(\hat{x}^C_e C^W_{z_{\dot{q}}} - 2C^W_{m_{\dot{q}}})\hat{s} \end{matrix} \end{bmatrix}$$

where $x^{C,P}$, $z^{C,P}$ are the coordinates of the pilot's center of mass P and of the cross tube-keel intersection C, respectively. Furthermore, s is the Laplace variable, the superscripts P and W in the aerodynamic coefficients indicate the pilot and wing subsystems, respectively, and the meaning of the other symbols is standard (e.g., see Ref. 5).

The transfer functions in the matrix $G(\hat{s})$ are thus numerically evaluated as a function of the wave number where $\hat{s} = j\Omega c_r/2$ and c_r is the reference chord. The load-factor response is also determined, once Eq. (2) is solved, as follows

$$G_n(s) = (\bar{n}'/\bar{\hat{u}}_g, \bar{n}'/\bar{\hat{w}}_g, \bar{n}'/\bar{\hat{q}}_g)^T = G^T(\hat{s})C(\hat{s}) \tag{3}$$

where

$$C = \begin{bmatrix} \cos\alpha_e\left[\dfrac{1}{u_\alpha}(C_{x_e} - C_{z_\alpha}) - 2\hat{u}_e C_{z_e}\right] + \sin\alpha_e\left[\dfrac{1}{u_\alpha}(C_{z_e} - C_{x_\alpha}) + 2\hat{u}_e C_{x_e}\right] + (C_{x_{\dot{\alpha}}} - C_{z_{\dot{\alpha}}})\hat{s} \\ \cos\alpha_e\left[\dfrac{1}{w_\alpha}(C_{x_e} - C_{z_\alpha}) - 2\hat{w}_e C_{z_e}\right] + \sin\alpha_e\left[\dfrac{1}{w_\alpha}(C_{z_e} - C_{x_\alpha}) + 2\hat{w}_e C_{x_e}\right] + (C_{x_{\dot{\alpha}}} - C_{z_{\dot{\alpha}}})\hat{s} \\ (C_{x_q}\sin\alpha_e - C_{z_q}\cos\alpha_e)\hat{s} - C_{z_{\dot{q}}}\hat{s}^2 \end{bmatrix} \frac{1}{C_w}$$

As a reference case, we consider the characteristics of the glider reported in Ref. 1. Let k be the reduced frequency. We observe that the phugoid natural frequency, although larger than the point approximation $k < 0.05$, is in the range of validity of the first-order approximation $k < 0.5$, provided

Received Nov. 30, 1990; revision received Nov. 1, 1991; accepted for publication Nov. 8, 1991.

*Research Assistant, Department of Mechanics and Aeronautics, via Eudossiana 18. Member AIAA.

that the unsteady motion is taken into account in the aerodynamics.[5]

The Bode plot reported in Fig. 1 shows the load-factor response [Eq. (3)] in the wave number range $\Omega = 10^{-2} - 10$. The value of $|\bar{n}'/\hat{w}_g|$ at low wave number, i.e., $\Omega = 0.01$ corresponding to a wavelength $\lambda = 376c_r$, represents the response to a gust nearly constant when compared to the dimension of the glider. If we consider a downgust $w_g = 6$ m/s with $V_e = 10.2$ m/s and a wing loading of 52.9 n/m^2, we have, from Fig. 1, $|\bar{n}'/\hat{w}_g| = 12.56$ dB and $n = 1 + n' = -1.46$. This result is consistent with that obtained in Ref. 3 by a simple model and for similar values of the parameters of the system. The load factor is such that the pilot is practically in free-fall and is unable to control the glider. However, as observed in Ref. 3, the time constant of the system is quite small and the high downward load persists only for a short period of time (0.3–0.5 s). The magnitude of $\bar{n}'/\hat{w}_g$ presents a peak at the phugoid frequency ($\Omega = 0.096$). By writing

$$\bar{m}'(\hat{s}) = k_1\bar{\alpha}'(\hat{s}) + k_2\bar{V}'(\hat{s}) + k_3\bar{\theta}'(\hat{s}) \tag{4}$$

where

$$\bar{\alpha}'(\hat{s}) = \bar{\hat{u}}'(\hat{s})/u_\alpha + \bar{\hat{w}}(\hat{s})/w_\alpha \tag{5}$$

$$\bar{V}'(\hat{s}) = \hat{u}_e\bar{\hat{u}}(\hat{s}) + \hat{w}_e\bar{\hat{w}}(\hat{s}) \tag{6}$$

$$k_1 = (C_{x_e} - C_{z_\alpha})\cos\alpha_e + (C_{z_e} - C_{x_\alpha})\sin\alpha_e + (C_{x_{\dot\alpha}} - C_{z_{\dot\alpha}})\hat{s} \tag{7a}$$

$$k_2 = 2(C_{x_e}\sin\alpha_e - C_{z_e}\cos\alpha_e) \tag{7b}$$

$$k_3 = (C_{x_q}\sin\alpha_e - C_{z_q}\cos\alpha_e)\hat{s} - C_{z_{\dot q}}\hat{s}^2 \tag{7c}$$

we can analyze the relative effect of angle of attack $\bar{\alpha}'$, flight speed $\bar{V}'$, and pitch angle $\bar{\theta}'$ on $\bar{n}'$. Figure 2 reports the vector components of $\bar{n}'/\hat{w}_g$ for $\Omega = 0.08$ and 0.1. We observe that the load-factor response depends mainly on the flight-speed term. In fact, in the angle-of-attack term, k_1 is relatively small due to $C_{z_{\dot\alpha}}$, and a relevant phase shift with respect to $\bar{n}'/\hat{w}_g$ is

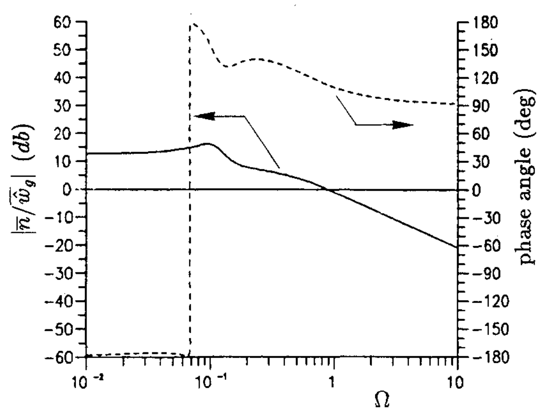

Fig. 1 Load-factor response to a vertical gust.

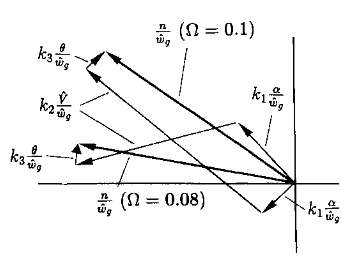

Fig. 2 Vector components of $\bar{n}'/\hat{w}_g$ for $\Omega = 0.08$ and 0.1.

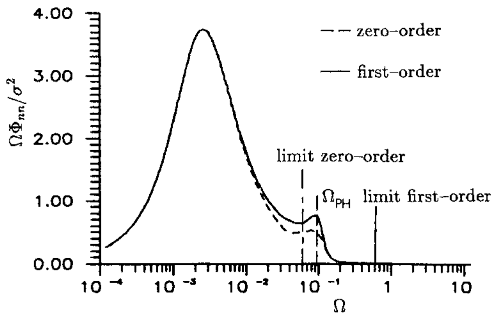

Fig. 3 PSD output of the load factor for the zero- and first-order approximations.

apparent for both the considered frequencies, i.e., a $\pi/4$ lead at $\Omega = 0.08$ and a $\pi/2$ lag at $\Omega = 0.1$.

At this point, after the solution of Eq. (2), the PDS output of the hang glider is evaluated as follows

$$\Phi_x = (\Phi_{uu}, \Phi_{ww}, \Phi_{\theta\theta})^T = \text{diag}(G^*\Phi_{x_g}G^T) \tag{8}$$

where an asterisk indicates the conjugate complex and the matrix of input spectra Φ_{x_g} is

$$\Phi_{x_g} = \begin{bmatrix} \Phi_{u_g u_g} & 0 & 0 \\ 0 & \Phi_{w_g w_g} & \Phi_{w_g w_{g_x}} \\ 0 & \Phi_{w_g w_{g_x}} & 0 \end{bmatrix}$$

As for the one dimensional spectra in the matrix Φ_{x_g}, it is apparent that the relatively low altitude of a hang-glider flight would lead to the application of a low-altitude turbulence model, in which the anisotropy of the turbulent velocity field is to be allowed for. Furthermore we see that, on the basis of the analysis given in Ref. 6, when the von Karman spectra are calculated at altitudes of $h = 200$ and 600 m, respectively, in the low-altitude turbulence spectra the energy density peaks at a value of the wavelength, which is nearly a decade larger than in the high-altitude case. This is relevant as far as the excitation of the high-frequency characteristic modes of the gliders is concerned, as we will see. However, the complexity associated to a low-altitude model is beyond the scope of the present analysis and, in this study, the high-altitude, first-order spectrum functions proposed in Ref. 7 have been used. They are

$$\Phi_{u_g u_g} = \frac{\sigma^2 L}{2\pi}\frac{k'}{1+k^2}(1+k'^2) \tag{9}$$

$$\Phi_{w_g w_g} = \frac{3\sigma^2 L}{2\pi}\frac{k'}{1+k^2}\left[\frac{k'^2}{3} + \frac{k^2}{1+k^2}\left(1 - \frac{k'^2}{3}\right)\right] \tag{10}$$

$$\Phi_{w_g w_{g_x}} = j\frac{3\sigma^2}{2\pi}\frac{kk'}{1+k^2}\left[\frac{k^2}{1+k^2} - \frac{k'^2}{3}\left(\frac{k^2}{1+k^2} - 1\right)\right] \tag{11}$$

where

$$k' = \frac{2\pi L/b}{[1 + k^2 + (2\pi L/b)^2]^{1/2}}$$

and, as usual, σ is the intensity, $L = 0.9h$ is the integral scale of the turbulence, $k = L\Omega$ is the dimensionless wave number, and b is the wing span.

The spectra of the output power are calculated from Eqs. (8–11) for $h = 600$ m, and use is made of Eqs. (3), (5), and (6) for the velocity, incidence, and load-factor transfer functions. In the range of considered frequencies and apart from the pitch angle output, in respect of which the system acts as a high-pass filter, we observe that the shape of the output spectra is slightly affected by the glider dynamics. However, in Fig. 3 the load-factor output presents a peak at the phugoid frequency, which is significant in spite of the fact that the turbulent energy is rather low in the range of frequencies of the characteristic modes of the aircraft. In this respect, the extension of the analysis to include a low-altitude turbulence model would probably lead to higher output energies for n. The same figure reports the limit of validity of the zero and first-order approximations and shows that the use of a zero-order model is satisfactory for wave numbers lower than 10^{-2}, but causes a 35% underestimate of the output of the load-factor power at resonance.

References

[1]de Matteis, G., "Dynamics of Hang-Gliders," *Journal of Guidance, Control, and Dynamics,* Vol. 14, No. 6, 1991, pp. 1145–1152.

[2]de Matteis, G., "Response of Hang-Gliders to Control," *Aeronautical Journal,* Vol. 94, No. 938, 1990, pp. 289–294.

[3]Jones, R. T., "Dynamics of Ultralight Aircraft: Motion in Vertical Gusts," NASA TM X-73228, April 1977.

[4]Kroo, I. M., "Aerodynamics, Aeroelasticity and Stability of Hang-Gliders," Ph.D. Thesis, Stanford Univ., Stanford, CA, 1983.

[5]Etkin, B., *Dynamics of Atmospheric Flight,* Wiley, New York, 1972, Chaps. 5, 13.

[6]Etkin, B., "Turbulent Wind and Its Effect on Flight," *Journal of Aircraft,* Vol. 18, No. 5, 1981, pp. 327–345.

[7]Etkin, B., "Theory of the Flight of Airplanes in Isotropic Turbulence—Review and Extension," AGARD Rept. 372, April 1961.

Thrust/Speed Effects on Long-Term Dynamics of Aerospace Planes

Gottfried Sachs*
Technische Universität München,
8000 Munich, Germany

Nomenclature

C_D = drag coefficient
C_L = lift coefficient
C_m = pitching moment coefficient
C_{m_i} = $2\partial C_m/\partial(i\bar{c}/V_0)$ where $i = q,\ \dot{\alpha}$
C_{N_V} = $\partial C_N/\partial(V/V_0)$ where $N = D,\ L,\ m$
C_{N_α} = $\partial C_N/\partial\alpha$ where $N = D,\ L,\ m$
C_{N_δ} = $\partial C_N/\partial\delta$ where $N = D,\ L,\ m$
$\bar{c}$ = mean aerodynamic chord
g = acceleration due to gravity
h = altitude
i_y = radius of gyration
k_ρ = $-g/(V_0^2\rho_h)$
M = Mach number
m = mass
n_h = thrust/altitude dependence, $n_h = (1/\rho_h)\partial(T/T_0)/\partial h$
n_V = thrust/speed dependence, $n_V = (V_0/T_0)\partial T/\partial V$
R = radius of the Earth
S = reference area
s_h = height mode root
T = thrust
V = speed
z_T = thrust-line offset
α = angle of attack (α_T for thrust)
Δ = denoting a perturbation, e.g., ΔV
δ = control (δ_e for pitch, δ_T for thrust)
μ = relative mass parameter, $\mu = 2m/(\rho S\bar{c})$
ρ = air density
ρ_h = density gradient, $\rho_h = (1/\rho)\mathrm{d}\rho/\mathrm{d}h$
σ = real part of a complex variable (σ_N for a zero, σ_p for phugoid)
ω_n = absolute value of a complex variable (ω_{n_N} for a zero, ω_{n_p} for a phugoid)

Received April 30, 1991; revision received June 10, 1991; accepted for publication June 24, 1991.

*Professor of Flight Mechanics and Flight Control. Associate Fellow AIAA.

Introduction

In recent papers,[1-6] the effect of thrust changes due to speed on long-term dynamics of vehicles in supersonic and hypersonic flight has been considered. The renewed interest in supersonic and hypersonic flight dynamics problems is the result of current aerospace plane programs in various countries like the German Sänger and the U.S. National Aerospace Plane (NASP) programs as well as others. It may also be stimulated by a better knowledge of the characteristics of propulsion systems proposed for hypersonic vehicles. Advanced air-breathing propulsion systems considered for application in supersonic and hypersonic flight are rather complex as regards their dependence of thrust on speed or Mach number.[1] They show significant variations in thrust throughout the Mach number range. These variations are due to the characteristics of an individual engine type used in a certain Mach number range like a turbojet, a ramjet, or a scramjet. They are also associated with changes in engine cycles when converting from one engine type to another.

For long-term dynamics, two types of thrust/speed effects are of importance. One may be termed a direct effect, which means thrust influence on force characteristics alone due to the change of thrust with speed. The other, which may be termed an indirect effect, is concerned with the influence of thrust on pitching moment due to thrust-axis offset and interaction with the flowfield. The direct effect of thrust/speed dependence has been considered in detail. For supersonic flight, it has been shown that this effect on the phugoid is small or even negligible.[5,6] By contrast, the height mode is rather sensitive as regards direct thrust/speed effects.[1-6] For indirect thrust/speed effects, pitching moment/speed sensitivity due to thrust-axis offset is considered to have an important long-period influence that may be significant even when the direct thrust/speed effects are small.[7,8]

The purpose of this Note is to provide more insight into thrust/speed effects on long-term modes of motion and to present new results for the hypersonic flight regime. Analytical considerations are presented to obtain results of a general nature. For both direct and indirect thrust/speed effects, it will be shown that there are significant differences in the sensitivities of the phugoid and height mode as regards such effects.

Aerospace Plane Dynamics

A thrust change with speed results in a force deviation from trim. In linearized form, thrust change may be expressed as

$$\Delta T/T_0 = n_V \Delta V/V_0 \qquad (1)$$

In case of a thrust-axis offset z_T, an aerodynamic pitching moment $(M_0)_{\text{aero}} = -T_0 z_T$ is necessary for trim. As a consequence, a deviation in pitching moment results when the trim state is disturbed. This indirect thrust/speed effect may be formulated as a nondimensional stability derivative

$$C_{m_V} = (n_V - 2)(z_T/\bar{c})C_D/\cos\alpha_T \qquad (2)$$

There may be additional thrust effects like an influence on the flowfield. They are considered to be included in C_{m_V}.

With the use of the expressions in Eqs. (1) and (2) for describing direct and indirect thrust/speed effects, the linearized equations of the longitudinal motion for a horizontal